Front. Optoelectron. 2016, 9(2): 330–337
DOI 10.1007/s12200-016-0619-y

RESEARCH ARTICLE

Simple dynamic energy core equivalent rays method to design freeform surface for extended source

Kun WANG, Yanjun HAN (✉), Hongtao LI, Yi LUO (✉), Zhibiao HAO, Lai WANG, Changzheng SUN, Bing XIONG, Jian WANG

Tsinghua National Lab on Information Science and Technology, Department of Electronic Engineering, Tsinghua University, Beijing 100084, China

Abstract A simple method is proposed to design freeform surface for Lambertian extended source. In this method, it can take advantage of the designing method for point source via substituting each incident ray with a dynamically calculated equivalent ray. For each facet on the freeform surface, the equivalent ray emits from the energy weighted average-emitting-position for the corresponding incident beam, and redirects into the direction which is determined by a source-to-target mapping. The results of the designing examples show that the light distributions' uniformities can be improved by this method, e.g., even the improvement of 59% can be achieved.

Keywords nonimaging optics, illumination design, light emitting diodes (LEDs)

1 Introduction

Light emitting diode (LED) source has the advantages of energy saving, long life time, and environmental friendly, etc. In lighting applications, optical freeform surfaces are usually required to redistribute the Lambertian distribution of LED into a prescribed distribution. When the point source assumptions [1] are valid for LED sources, the freeform surface designing problems can be solved accurately with the well developed methods [2–7]. In these methods [2–7], the deflective directions of the incident rays are determined according to a specific one-to-one mapping between the source angle grids and the target grids based on energy conservation. Whereas, if the point source assumptions are invalid (e.g., the compactness ratio of the freeform surface's height to the source diameter is less than five [8]), a light distribution degradations would occur if the freeform surfaces are designed by the methods for point source [1]. In these cases, LED sources are necessary to be considered as Lambertian extended sources, and their freeform surfaces designing ideas are usually quite different to the energy conservative source-to-target mapping idea of the point source cases.

For example, simultaneous multiple surface (SMS) method [9] is designing two freeform surfaces simultaneously through accurately controlling two edge wave fronts. Tailored edge-ray design method [10,11] is based on the edge-ray principle [12], and the freeform surface is constructed by controlling two edge rays. The iterative feedback compensation method [13–15] modifies the prescribed light distribution according to the simulated result, and iterates the process for a number of times to obtain a satisfying result. Besides, some other methods are based on optimizations [16–18]. Moreover, it seems that the freeform surface designing for extended source in the generalized functional method [7] has a pre-determined one-to-one mapping based on energy conservation among the source positions, the target directions, and the points on the freeform surface profile. However, the extended source in this method has a precondition that its etendue is zero [13], and the feedback compensation method would be added to deal with the Lambertian extended source cases (nonzero-etendue source cases) [13].

The proposed method can design freeform surface for Lambertian extended source, which is named as energy core equivalent rays (ECER) method. During the freeform surface construction, though in this method it takes advantage of the source-to-target mapping of the point source case, the emitting position of each ray is calculated dynamically instead of pre-determined, and there is no necessity to have a one-to-one correspondence between the source positions (where the equivalent rays emit from) and the points on the freeform surface profile.

Received February 2, 2016; accepted February 18, 2016

E-mail: yjhan@tsinghua.edu.cn, luoy@tsinghua.edu.cn

2 ECER method

2.1 Principle of the ECER method

As a contrast, Fig. 1(a) shows a rotational symmetry optical system which aims to achieve a prescribed illumination distribution on a target plane when using a point source. The θ angles represent the source angle grids, and r represent the corresponding location on the meshes of the target area, a prescribed $\theta \sim r$ mapping can be determined based on energy conservation, and each point (facet) on the freeform surface (corresponds to a specific θ angle) would only receive one incident ray and emits one outgoing ray. Then a suitable normal vector for each freeform surface facet can be determined by Snell's Law, and the freeform surface for point source can be constructed. In an intensity distribution designing problem, the designing process is similar, which is usually using a $\theta \sim \gamma$ mapping, where γ is defined as the angle between the direction of the rotational symmetry axis and the directions of the emergent rays.

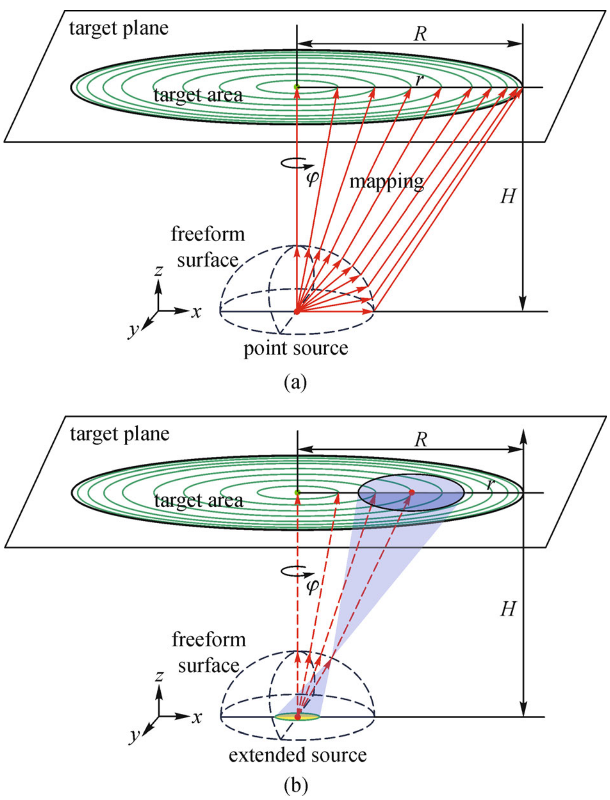

Fig. 1 (a) Illustration of a $\theta \sim r$ mapping for point source; (b) when the source is an Lambertian extended source, each facet of the freeform surface will form a light spot

However, when the dimension of the source is increasing and the source should be considered as a Lambertian extended source, as shown in Fig. 1(b), each facet on the freeform surface would receive an incident beam from the extended source instead of a ray, and form a light spot on the target plane. If the freeform surface in Fig. 1(b) is the same as in Fig. 1(a), only the ray emitted from the source center (the origin of the source angle grid) can be redirected onto the corresponding mapping-location on the target area, and the paths of the other incident rays would deviate from the mapping regulation.

As illustrated in Fig. 2, assuming that the position of a certain freeform surfacet facet is $p_f = (x_f, y_f, z_f)$ and its corresponding normal vector is $\boldsymbol{N}_f$, the normal vector of the source is $\boldsymbol{N}_s$, and then the energy carried by the incident ray which is emitted from the source position $(x_s, y_s, 0)$ can be calculated by Eq. (1).

$$\Phi(p_f, \boldsymbol{N}_f, x_s, y_s) = ds \cdot L \cdot \cos\alpha \cdot \cos\beta \cdot df / d^2, \tag{1}$$

Where, ds is the area of the small source facet whose center position is $(x_s, y_s, 0)$, L is the luminance which is a constant for a Lambertian source, α is the included angle between $\boldsymbol{N}_s$ and this incident ray vector, β is the included angle between $\boldsymbol{N}_f$ and this incident ray vector, df is the area of the small facet on the freeform surface whose center position is p_f, d is the distance between the positions $(x_s, y_s, 0)$ and p_f. The parameters α, β and d are usually quite different for the rays emitted from different source positions.

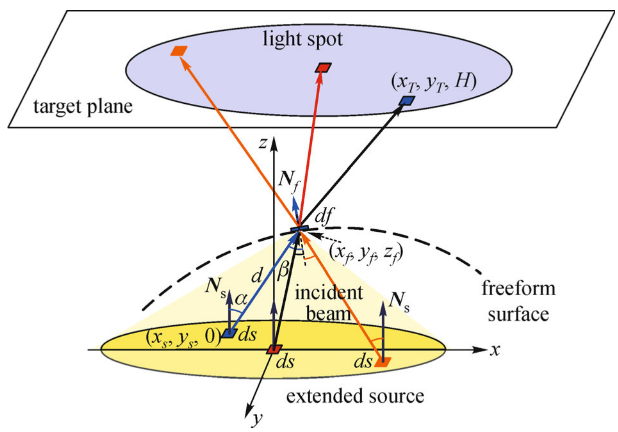

Fig. 2 An incident beam is formed by a large number of rays, which are emitting from different source positions and passing through a specific small facet of freeform surface

As for a facet on the freeform surface profile, due to the energy carried by each rays within the incident beam are usually not uniformly distributed, the ray emitted from the source center cannot always be the best one to represent the incident beam, therefore, it is reasonable to find a more suitable ray to represent the incident beam. ECER can be calculated for the incident beam by computing the ray's average emitting position on the source as Eq. (2), where the energy carried by a ray could be the weight. To some degree, this calculation is similar to the way of calculating a centroid.

$$\begin{cases} x_{\mathrm{ECER}}(p_f,\boldsymbol{N}_f)=\dfrac{\iint\limits_{As} x_s\cdot f(p_f,\boldsymbol{N}_f,x_s,y_s)\cdot \mathrm{d}x_s\mathrm{d}y_s}{\iint\limits_{As} f(p_f,\boldsymbol{N}_f,x_s,y_s)\cdot \mathrm{d}x_s\mathrm{d}y_s}, \\ y_{\mathrm{ECER}}(p_f,\boldsymbol{N}_f)=\dfrac{\iint\limits_{As} y_s\cdot f(p_f,\boldsymbol{N}_f,x_s,y_s)\cdot \mathrm{d}x_s\mathrm{d}y_s}{\iint\limits_{As} f(p_f,\boldsymbol{N}_f,x_s,y_s)\cdot \mathrm{d}x_s\mathrm{d}y_s}, \end{cases} \tag{2}$$

where, the integral range As is the area of the extended source; the formula of the energy weight $f(p_f,\boldsymbol{N}_f,x_s,y_s)$ represents for the transition energy $\Phi(p_f,\boldsymbol{N}_f,x_s,y_s)$ which is given in Eq. (1). If the extended source is pre-divided into equal-area small source facet, then ds would be a constant as L and df (for a certain freeform surface facet), and the three parameters can be eliminated from Eq. (2). Therefore, $f(p_f,\boldsymbol{N}_f,x_s,y_s)$ can be simplified into Eq. (3), and $f(p_f,\boldsymbol{N}_f,x_s,y_s)$ is zero when $\beta\geqslant\theta_{\mathrm{TIR}}$, which means that the ray encounters the total internal reflection would not be considered, and θ_{TIR} is the total internal reflection angle of the optical system.

$$\begin{cases} f(p_f,\boldsymbol{N}_f,x_s,y_s)=\cos\alpha\cdot\cos\beta/d^2, & \beta<\theta_{\mathrm{TIR}}, \\ f(p_f,\boldsymbol{N}_f,x_s,y_s)=0, & \beta\geqslant\theta_{\mathrm{TIR}}. \end{cases} \tag{3}$$

The ECER for a freeform surface facet needs to be calculated dynamically. On one hand, the normal $\boldsymbol{N}_f$ for a freeform surface facet is eventually ascertained according to the following criterion: since the normal of any facet on the freeform surface could only accurately control one ray obeying the source-to-target mapping, let the normal of the freeform surface facet redirect the ECER ray into the mapping location. On the other hand, as shown in Eq. (2), the calculation for the emitting position of ECER$(x_{\mathrm{ECER}},y_{\mathrm{ECER}},0)$ also needs the information of $\boldsymbol{N}_f$. As a matter of fact, using a small number of iterations within the calculation for each specific freeform surface facet, the $\boldsymbol{N}_f$ and $(x_{\mathrm{ECER}},y_{\mathrm{ECER}},0)$ can be ascertained simultaneously.

In Fig. 3, $\mathrm{d}r_1,\mathrm{d}r_2$ represent for the mapping location on the target plane for the specific θ angles, which are pre-determined, and N_{f1} and N_{f2} are the corresponding normal vectors of the freeform surface facet. As a comparison, Fig. 3(a) shows the freeform surface designing case for point source, and Fig. 3(b) shows the freeform surface construction process with ECER method. The difference within the two cases is that it is using the dynamically calculated ECER to substitute the incident ray which emits from the point source (source center). Moreover, it can be proved that the emergent ray of an ECER also corresponds to the energy weighted average location of the light spot on the target plane.

2.2 Designing process of ECER method

To design a rotational symmetry optical system, the flow chart of the process is shown in Fig. (4). Comparing with the method for point source, the difference in ECER method is mainly within the following 4-th item.

1) Define the dimensional parameters of the optical system as well as the refractive index, etc.

2) Compel a point source assumption for the source, establish the one-to-one source-to-target mapping ($\theta\sim r$ mapping for the illuminance designing case, or $\theta\sim\gamma$ mapping for the intensity designing case) based on energy conservation.

3) Assuming k is the index of the points on the freeform surface contour, which corresponds to a certain θ angle. The position $p_f(k=1)$ and the normal vector $\boldsymbol{N}_f(k=1)$ of the freeform surface profile start point (facet) are given. The number of the points (facets) which construct the freeform surface profile is L.

4) When calculating the freeform surface profile, except the condition $k=1$, the position of the k-th point (facet) $p_f(k)$ is geometrically determined by $p_f(k-1)$ and $\boldsymbol{N}_f(k-1)$ (the geometrical construction way has been described in Ref. [6]). The way to ascertain the normal vector $\boldsymbol{N}_f(k)$ for the k-th point (facet) by ECER method is illustrated in the dashed box in Fig. 4, which includes the numeric iterations. Preliminarily, taking $\boldsymbol{N}_f(k-1)$ as $\boldsymbol{N}_f(k)$, then

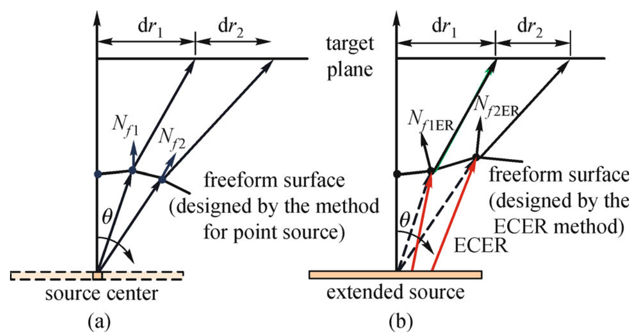

Fig. 3 (a) Construction of the freeform surface contour for point source; (b) ECER method is using the equivalent ray to substitute the incident ray from the point source during each facet construction, and each equivalent ray is obtained by several times iteration

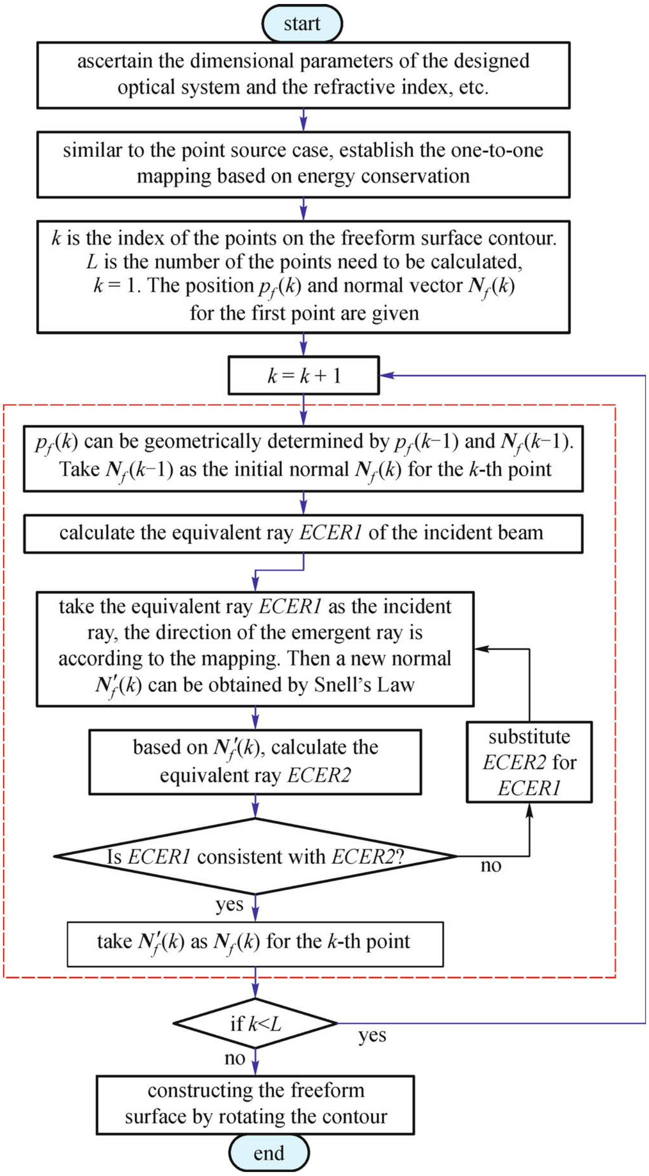

Fig. 4 Flow chart of the ECER method

an *ECER1* can be calculated as a preliminary incident ray, and its emergent ray's direction is determined by the source-to-target mapping, then a new normal vector $N_f'(k)$ can be obtained by Snell's Law. Then based on $N_f'(k)$, an *ECER2* can be newly calculated as the incident ray. If the emitting positions of *ECER1* and *ECER2* are not consistent with each other, substituting *ECER2* for *ECER1*, and a new normal $N_f'(k)$ would be determined again in the same way, and the old one would be substituted. The iterations would be finished until the emitting positions of *ECER1* and *ECER2* are consistent with each other, then the normal $N_f'(k)$ would be the eventual $N_f(k)$ for the k-th point (facet) of the freeform surface profile. In this process, the calculation only needs a small number of iterations, and the calculating time would usually be only hundreds milli-seconds.

5) $k = k + 1$, and repeat the above process 4 until $k = L$, then construct the freeform surface by rotating the profile.

3 Designing examples and results

3.1 To achieve uniform illuminance distribution with extended source

A refractive freeform surface for a Lambertian extended source is designed to achieve a circular uniform illuminance distribution in the target area whose radius is R. Assuming the energy within the target area is equal to the energy emitted from the source in 2π solid angle ($\theta \in [0,\pi/2]$), then the mapping of $r(\theta)$ can be obtained as $r(\theta) = R \cdot \sin\theta$ under the point source approximation.

Assuming the height of the designed freeform surface (h) is 20 mm, the target area radius R = 1000 mm, the height of the target plane (H) which is paralleled to the source plane is 1000 mm, the refractive index of the lens is 1.49. The freeform surfaces are designed for the Lambertian sources whose radius (r_s) are 2, 3, 4, 5 mm, respectively. In Table 1, it shows the contrasts between the results achieved by ECER method and the traditional method (named as the method that the freeform surface is designed for point source but applied to extended source directly), and the results are simulated by Monte Carlo ray tracing method with tracing one million rays. The relative standard deviation (RSD) values and energy utilization ratios η of the illuminance distributions achieved by the two methods are listed in Table 1, where the improvements and variations are included as well. η is defined as the ratio of the energy within the target area to the energy emitted from the source.

Table 1 Results of this uniform-illuminance-distribution designing example

source radius r_s/mm	traditional method		ECER method		variation in η (percentage points)	improvements in RSD
	η	RSD	η	RSD		
2	96.4%	0.240	94.4%	0.207	2.0	13.8%
3	92.3%	0.313	89.4%	0.253	2.9	19.2%
4	87.6%	0.378	84.4%	0.290	3.2	23.3%
5	84.8%	0.413	80.3%	0.332	4.6	19.6%

Comparing with the traditional method, the ECER method can improve the uniformity of the illuminance distribution for all these four cases as shown in Table 1. Take the 3 mm radius case as an example, the RSD value is improved by 19.2%, and the η is only decreased by 2.9 percentage point, and Fig. 5(a) is the illuminance distribution on the target plane achieved by the traditional method, and Fig. 5(b) shows the illuminance distribution achieved by ECER method, where both the dotted circles marked the boundaries of the target area. Figure 5(c) is the line chart of the illuminance distribution corresponded to Fig. 5(a), and Fig. 5(d) is the line chart of the illuminance distribution corresponded to Fig. 5(b). An improvement of the light distribution uniformity can be directly observed.

In Fig. 5(e), it depicts the x coordinates of the ECER emitting positions for each facet of the freeform surface profile which corresponds to one of the θ angles (the y and z coordinates of the ECER emitting positions are zero). In the traditional method, the emitting positions of the incident rays are always the source center. Moreover, it can be noticed that the emitting positions of ECERs and the facets on the optical-surface profile do not have one-to-one correspondence.

From Table 1, it can be observed that the RSD value is increased as r_s increased, e.g., in the case $r_s = 5$, RSD is higher than 0.3. The explanations are as following: the increasing of the source size would lead to an increasing of the dimensions of the light spots, when the light spots dimensions are prone to be expanded relatively large and comparable to the size of the target area, it is very hard to discern the relations between the light spots' expanded locations and their corresponding exact locations according to the source-to-target mapping, therefore it is hard to take advantage of the mapping, then the effectiveness of the method would be fading in this case.

3.2 To achieve uniform intensity distribution with extended source

A refractive freeform surface for a Lambertian extended source is designed to achieve the uniform intensity in the γ angle range of $0° - 60°$. Assuming the outgoing energy within the solid angle that $\gamma \in [0,\pi/3]$ is equal to the incident energy emitted from the source within 2π solid angle ($\theta \in [0,\pi/2]$), then the relationships of $\gamma(\theta)$ can be obtained as $\gamma(\theta) = \arccos(0.75 + 0.25 \cdot \cos 2\theta)$ under the point source approximation.

The refractive index of the lens is 1.49. The height of the central point on the freeform surface (h) is 20 mm. The outgoing angle of the optical system is relatively large, then the Lambertian source radius (r_s) can be chosen from a large range, where the radius of 3, 5, 7, 10 and 12 mm is applied, respectively. In Fig. 6, it shows the contrasts between the results achieved by the ECER method and the traditional method (defined similarly as the above example). The results are simulated by Monte Carlo ray

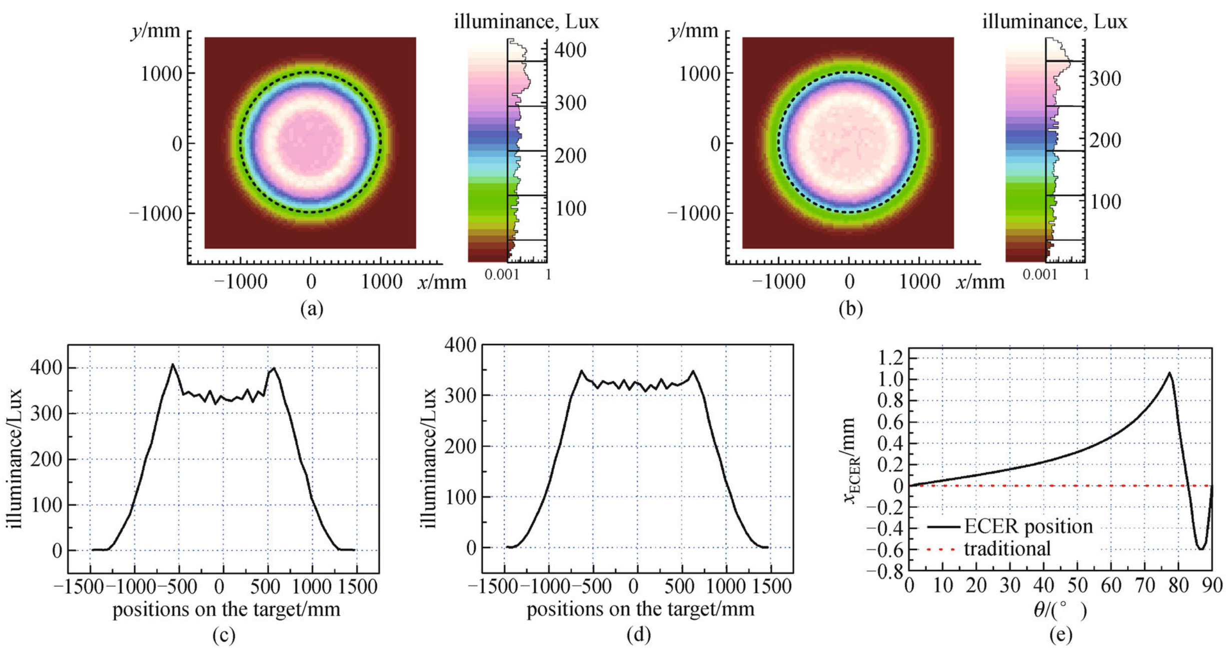

Fig. 5 When the source radius is 3 mm in the designing example, (a) illuminance distributions achieved by the traditional method; (b) illuminance distributions achieved by ECER method; (c) line chart of the illuminance distributions achieved by the traditional method; (d) line chart of the illuminance distributions achieved by ECER method, (e) x coordinates of the ECER emitting positions for each facet of the freeform surface profile

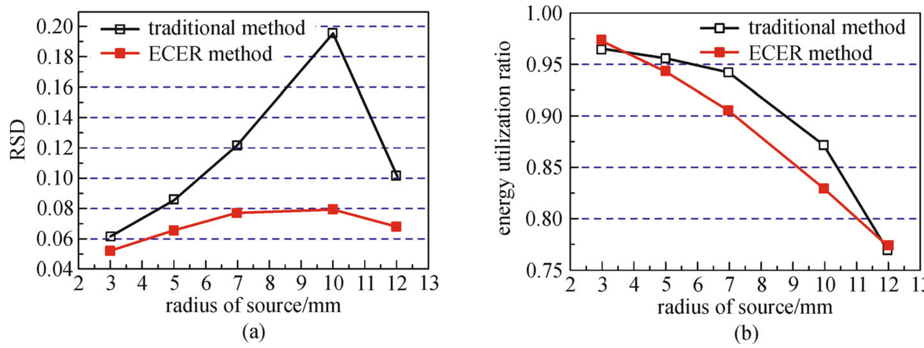

Fig. 6 Results of the intensity distributions of the optical systems which are designed by ECER method and the traditional method, respectively. (a) RSD values of the intensity distributions; (b) energy utilization ratio of the intensity distributions

tracing method with tracing one million rays. Figure 6(a) is the RSD value of the intensity distributions with different source radius. Comparing with the traditional method, it is noticed that the ECER method can generally improve the uniformity of the intensity distribution. Figure 6(b) shows the energy utilization ratio η of these intensity distributions, where η is defined as the ratio of the energy within the target solid angle to the energy emitted from the source.

Table 2 lists the RSD values and η of each intensity distributions, as well as the improvements and variations. When the source radius is changed from 3 to 12 mm, the RSD values of the intensity distributions achieved by ECER method are all having considerable improvements and less than 0.1, while the corresponding η are near that of the traditional method. It can be noticed that the RSD value can be even improved by as highly as 59.0% when the source radius is 10 mm, while η is only decreased by 4.3 percentage point.

For the case that the source radius is 10 mm, Fig. 7(a) gives the achieved intensity distributions which are designed with ECER method, and Fig. 7(b) gives the intensity distributions achieved by the traditional method, where the radial directions of the charts are the increasing variations directions of the angle γ from 0° to 60°. To observe the comparison more clearly, Fig. 7(c) is the line charts of the two intensity distributions along the γ angle, which can indicate the uniformity improvement is conspicuously occurred with the ECER method. Figure 7(d) shows the corresponding lens designed by ECER method.

4 Conclusions

The ECER method has the advantages of simplicity and convenience to design freeform surface for Lambertian extended source. In this method, an equivalent ray is dynamically calculated for each freeform surface facet by energy-weighted-average calculations, and the incident ray is substituted with the equivalent ray instead of the ray emitted from the source center. This method can improve the uniformity of the achieved light distributions as shown in the results. For example, in the case which is achieving a uniform intensity distribution in the angle that $\gamma \in [0,\pi/3]$, comparing with the traditional method, the ECER method can improve the RSD value by 59.0% when the radius of the source is 10 mm and the height of the freeform surface is 20 mm, while the energy utilization ratio is only decreased by 4.3 percentage points.

The ECER method is effective to obtain favorable results in the cases which have a relatively small source size or the emergent solid angle of the target area is relatively large. When designing for a specific case for extended source, on account of its simplicity and its

Table 2 Results of this uniform-intensity-distribution designing example

source radius r_s/mm	traditional method		ECER method		variation in η (percentage points)	improvements in RSD
	η	RSD	η	RSD		
3	96.5%	0.062	97.2%	0.052	enhanced by 0.7	16.1%
5	95.5%	0.086	94.3%	0.065	decreased by 1.2	24.4%
7	94.2%	0.122	90.5%	0.077	decreased by 3.7	36.9%
10	87.2%	0.195	82.9%	0.080	decreased by 4.3	59.0%
12	76.9%	0.101	77.3%	0.068	enhanced by 0.4	32.7%

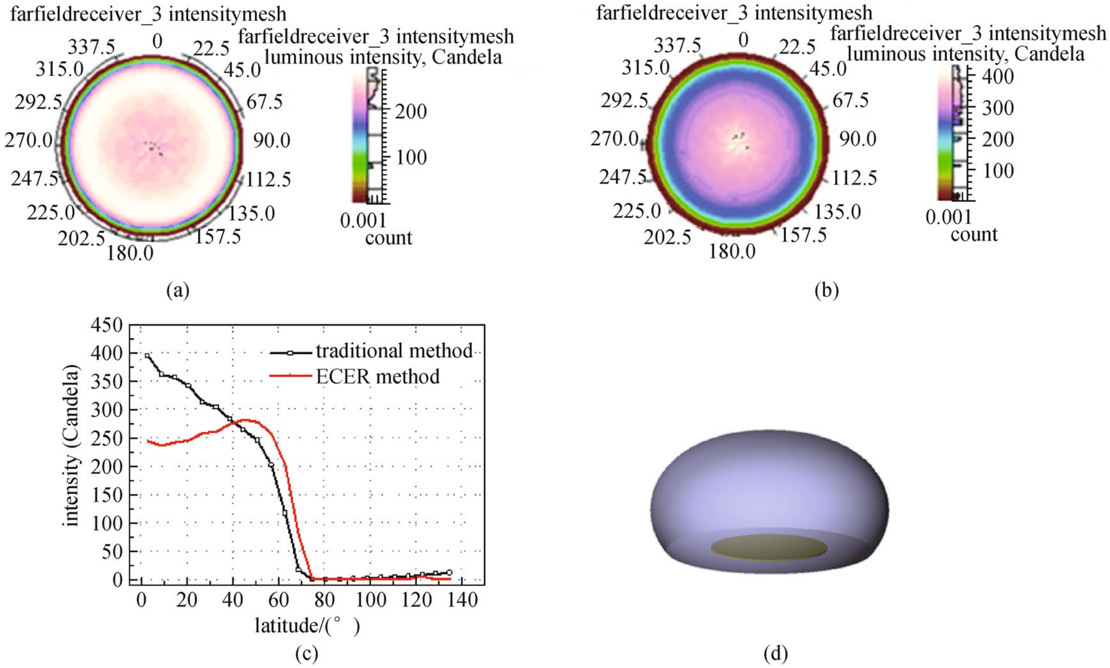

Fig. 7 When the source radius is 10 mm, (a) intensity distributions designed with ECER method; (b) intensity distributions designed with the traditional method; (c) line chart of the two intensity distributions; (d) designed lens shape by ECER method and the source

connection to the designing methods for point source, it could be suggested to design the freeform surface by ECER method first as an attempt to get the more favorable results.

Acknowledgements This work was supported by the National Key Basic Research Program of China (Nos. 2015CB351900, 2011CB301902 and 2011CB301903), the National Key Technology Research and Development Program of the Ministry of Science and Technology of China (No. 2012BAE01B03), the Science and Technology Planning Project of Guangdong Province (No. 2011A081301003), the Opened Fund of the State Key Laboratory on Integrated Optoelectronics (No. IOSKL2012KF09), the High Technology Research and Development Program of China (Nos. 2011AA03A112, 2011AA03A106 and 2011AA03A105), the National Natural Science Foundation of China (Grant Nos. 61307024, 61176015 and 61176059).

References

1. Kari T, Gadegaard J, Søndergaard T, Pedersen T G, Pedersen K. Reliability of point source approximations in compact LED lens designs. Optics Express, 2011, 19(S6): A1190–A1195
2. Wu R, Xu L, Liu P, Zhang Y, Zheng Z, Li H, Liu X. Freeform illumination design: a nonlinear boundary problem for the elliptic Monge-Ampére equation. Optics Letters, 2013, 38(2): 229–231
3. Parkyn W A. Design of illumination lenses via extrinsic differential geometry. Illumination and Source Engineering, 1998, 3428: 154–162
4. Ries H, Muschaweck J. Tailored freeform optical surfaces. Journal of the Optical Society of America A, Optics Image Science and Vision, 2002, 19(3): 590–595
5. Oliker V. Geometric and variational methods in optical design of reflecting surfaces with prescribed irradiance properties. In: Proceedings of SPIE, International Society for Optical Engineering. 2005, 594207
6. Wang L, Qian K, Luo Y. Discontinuous free-form lens design for prescribed irradiance. Applied Optics, 2007, 46(18): 3716–3723
7. Bortz J, Shatz N. Generalized functional method of nonimaging optical design. In: Proceedings of SPIE, Nonimaging Optics and Efficient Illumination Systems III. 2006, 6338: 633805
8. Wester R, Müller G, Völl A, Berens M, Stollenwerk J, Loosen P. Designing optical free-form surfaces for extended sources. Optics Express, 2014, 22(S2): A552–A560
9. Benítez P, Miñano J C, Blen J, Mohedano R, Chaves J, Dross O, Hernández M, Falicoff W. Simultaneous multiple surface optical design method in three dimensions. Optical Engineering, 2004, 43 (7): 1489–1502
10. Ries H R, Winston R. Tailored edge-ray reflectors for illumination. Journal of the Optical Society of America A, 1994, 11(4): 1260–1264
11. Ong P T, Gordon J M, Rabl A, Cai W. Tailored edge-ray designs for uniform illumination of distant targets. Optical Engineering, 1995, 34(6): 1726–1737
12. Davies P A. Edge-ray principle of nonimaging optics. Journal of the Optical Society of America A, 1994, 11(4): 1256–1259
13. Bortz J, Shatz N. Iterative generalized functional method of nonimaging optical design. In: Proceedings of the Society for Photo-Instrumentation Engineers. 2007, 6670: 66700A

14. Luo Y, Feng Z, Han Y, Li H. Design of compact and smooth free-form optical system with uniform illuminance for LED source. Optics Express, 2010, 18(9): 9055–9063
15. Cassarly W J. Iterative reflector design using a cumulative flux compensation approach. In: Proceedings of SPIE, International Optical Design Conference. 2010, 7652(4): 76522L
16. Wang K, Han Y, Li H, Luo Y. Overlapping-based optical freeform surface construction for extended lighting source. Optics Express, 2013, 21(17): 19750–19761
17. Zhang W Z, Liu Q X, Gao H F,Yu F H, Free-form reflector optimization for general lighting. Optical Engineering, 2010, 49(6): 063003
18. Mao X L, Li H T, Han Y J, Luo Y. A two-step design method for high compact rotationally symmetric optical system for LED surface light source. Optics Express, 2014, 22(S2): A233–A247

Kun Wang received her Ph.D. degree in electronic engineering from Tsinghua University, Beijing, China, in 2015. She received her B.S. degree from the Xidian University in 2009. Her research presently focuses on the LED lighting devices designing, especially the freeform surface designing method for extended source.

Yanjun Han received his Ph.D. degree in electronic engineering from Tsinghua University, Beijing, China, in 2003. Since 2003, he has been a lecturer in the Department of Electronic Engineering, Tsinghua University, where he is now an associate professor. His research interest has been in the area of solid-state lighting.

Hongtao Li received his B.S. degree in optical information science and technology from Shandong University, Jinan, China, in 2003, and Ph.D. degree in physical electronics and optoelectronics from Tsinghua University, Beijing, China, in 2008. Since 2008, he has been working as a Faculty Member of the Department of Electronic Engineering, Tsinghua University, and now he is an associate professor. His current research interests include non-imaging optics, solid state lighting, and flexible and stretchable optoelectronics.

Yi Luo is a professor and the director of Tsinghua National Laboratory on Information Science and Technology, at the Department of Electronic Engineering, Tsinghua University, Beijing, China. He received his Ph.D. degree in the Department of Electronic Engineering, University of Tokyo, Japan, in 1990. His main research fields are optoelectronics devices and nonimaging optics for luminaries based on white LEDs.

Zhibiao Hao received his Ph.D. degree in physical electronics from Tsinghua University in 2002, then he joined Tsinghua University and now is a Professor at the Department of Electronic Engineering. He worked as a visiting scholar in University of California, Los Angeles, from 2006 to 2007. His current research interests include molecular beam epitaxy of compound semiconductors and nanostructure optoelectronic devices.

Lai Wang received his B.S. and Ph.D. degrees from Tsinghua University (THU), China, in 2003 and 2008, respectively, both in electronic engineering. He joined the faculty at THU as an Assistant Professor in the Department of Electronic Engineering in 2008. His research presently focuses on III-nitride materials and devices.

Changzheng Sun received his B.S., M.S., and Ph.D. degrees from Tsinghua University, Beijing, China, in 1995, 1997, and 2001, respectively, all in physical electronics and optoelectronics. Since 2001, he has been working as a faculty member of Department of Electronic Engineering, Tsinghua University, Beijing, China. His current research interests include device physics and fabrication technology of high-speed optoelectronic devices for fiber communications and radio-over-fiber wireless links.

Bing Xiong is an associate professor at the Department of Electronic Engineering, Tsinghua University, Beijing, China. He received his Ph.D. degree in the Department of Electronic Engineering, Tsinghua University, in 2005. His main research fields are high speed modulators and photodetectors for information optoelectronics.

Jian Wang received his B.S., M.S., and Ph.D. degrees from Tsinghua University, Beijing, China, in 1999, 2002, and 2005, respectively, all in the Deptartment of Electronic Engineering. In 2005, he joined Deptartment of Electronic Engineering, Tsinghua University, as a Faculty Member. In 2011, he became an associate researcher. His research activities include solar energy, field emission display, and high-speed optoelectronic devices.